The Effect of H_3O^+ on the Structure and Dynamics of Water at the Interface with Phospholipid Bilayers

Evelyne Deplazes[1,2*], Farzaneh Sarrami[3], David Poger[4],

[1] School of Life Sciences, University of Technology Sydney, Ultimo, NSW 2007, Australia.

[2] School of Pharmacy and Biomedical Sciences, Curtin Institute for Computation, Curtin University, Perth, WA 6845, Australia.

[3] School of Chemistry and Biochemistry, The University of Western Australia, Perth, WA 6009, Australia

[4] School of Chemistry and Molecular Biosciences, The University of Queensland, Brisbane QLD 4072, Australia.

*Corresponding author: evelyne.deplazes@uts.edu.au. +61 2 9514 2000

Abstract

This study investigates the effect of hydronium ions (H_3O^+) ions on the structure and dynamics for water at the interface of a phospholipid bilayer using molecular dynamics (MD) simulations of a POPC bilayer in the presence and absence of H_3O^+ ions. From these simulations, the survival probability, hydrogen bond lifetimes, orientation relaxation and angular distribution of interfacial water, at increasing distances from the membrane surface, were calculated. Simulations of POPC in the absence of H_3O^+ ions reproduce previously reported deviations of interfacial water from the properties of bulk water. Our results show that in the presence of H3O+ these deviations are even more pronounced with the strongest effects seen in the survival probability and orientational relaxation. To further investigate the effect of the H_3O^+ -induced reduction of area per lipid on interfacial water, we carried out simulations where H_3O^+ ions were removed but the area per lipid was fixed to the values seen the presence of H_3O^+. The combined findings from our study suggest that the presence of H_3O^+ ions affects the properties of interfacial water, accentuates the deviation from bulk properties and extends the long-range effect of these deviations further away from the membrane surface.

Introduction

Biological membranes are semipermeable barriers that separate the cell from its external environment and compartmentalise cellular organelles. Membranes are critical for numerous physical processes including the active and passive diffusion of molecules, as well as the structure and function of membrane proteins. Phospholipid bilayers form the main component of cell membranes and consequently, any membrane-mediated process is affected by the structure, mechanical and physico-chemical properties of the bilayer. There is also an increasing number of studies demonstrating the importance of water in the structure and dynamic of membranes and phospholipid bilayers [1-2]. Rather than being a mere solvent driving the hydrophobic effect, water at the water-lipid interface should be "considered as a component of the membrane" that acts a "connecting material" affecting the structure and thus function of membranes [2]. The structure and dynamics of such interfacial water has been studied using a wide range of techniques [3-7]. The combined results from these studies suggest that interfacial water has distinct properties that differ from the ones of bulk water. More specifically, interfacial water appears to have shorter and longer-lived hydrogen bonds[3, 8-10] and a preferred orientation of the water dipole [11-16] that might further depend on the nature of the lipid [17]. As a result of the interaction with lipid head groups, interfacial water exhibits reduced rotational motion (i.e. slower re-orientational relaxation) [18-22] and altered diffusion [8, 13, 20, 23-24]. It appears that interfacial water is a compromise of the water adopting the network-like structure of the bulk and arranging itself to optimise its direct interaction with the lipid headgroups [2].

The structure, morphology and physico-chemical properties of a phospholipid bilayer is also strongly affected by its lipid composition and environmental factors such as temperature, pressure and ionic strengths. These effects have been studied extensively using a wide range of wet-lab and simulation techniques [25-31]. Less studied is the effect of pH on membranes. A few studies have shown that lowering the pH of the bathing solution affects the mechanical and electrical properties of phospholipid bilayers [32] and increase the lamellar gel-to-liquid crystalline phase-transition temperature [33]. In addition, both increases and decrease in pH cause changes in membrane conductivity and alter water penetration into the bilayer. Subsequently, this changes the area per lipid (APL)

and membrane thickness [34-35]. Variations in the pH also alters capacitance and interfacial tension [36-37]. Given the dependence of interfacial water on bilayer properties, it is likely that pH also affects structure and dynamics of water at the membrane surface.

A process that is related to both pH and interfacial water is the movement of solvated protons across the membrane surface required for cellular respiration and energy metabolism. The membrane-facilitated migration of protons has been studied for decades, using both complex biological membranes as well as model membranes such as phospholipid bilayers and vesicles [38-41]. While the detailed mechanism of proton migration is still not fully understood, many studies suggest that interfacial water is integral to proton migration by forming a structural, kinetic and/or energetic barrier that prevents solvated protons to escape into the bulk [39, 42-45]. This suggest that proton migration is closely linked to the unique properties of interfacial water. Studies of proton migration on membrane surface and the effect of pH on membranes clearly highlights the complex interplay between the lipid bilayer, interfacial water and surface-bound ions [46].

Solvated protons at the membrane surface can exist in a number of forms including the hydronium cation (H_3O^+), the Zundel cation ($H_5O_2^+$) and the Eigen cation ($H_9O_4^+$). The affinity of these ions for membrane surfaces has been demonstrated using both 'wet-lab' experiments [47-50] and simulations [35, 51-53]. The latter have played an important role in providing a molecular level insight into the mechanism of how solvated protons bind to membrane surfaces. Combined insight from these studies indicate that hydronium and Zundel cations displace water at the membrane surface, and that the cations reside in the 'binding sites' formed by neighbouring lipids [51-54]. A recent simulation study [35] showed that at high hydronium concentrations these hydronium-lipid interactions are directly linked to the reduction in APL and increase in membrane thickness observed in neutron scattering experiments of membranes at low pH.

In the present study, we investigate the effect of the accumulation of hydronium ions at the water-lipid interface on interfacial water. Specifically, we use simulations of 1-Palmitoyl-2-oleoyl-*sn*-glycero-3-phosphocholine (POPC) at neutral conditions and in the

presence of 40 mM H_3O^+ to assess the effect of hydronium-lipid and hydronium-water interaction on the structure, dynamics and hydrogen bonding properties of interfacial water.

Methods

The detailed setup of the simulation systems as well as the parameters for the MD simulations were reported previously [35] and are thus only briefly outlined below.

Model systems for membrane and 'bulk water'

Both membrane and bulk water simulations were carried out in the absence and presence of H_3O^+ (Table 1). The systems referred to as 'neutral' contained no H_3O^+ ions while the 'low pH' systems contained H_3O^+ ions equivalent to a concentration of 0.04 M, denoted as 40 mM [H_3O^+]. The concentration is calculated based on the ratio of water molecules and H_3O^+ ions and the water concentration of 55.5 M. The membrane systems consisted of a pre-equilibrated bilayer of 512 POPC molecules and approximately 23,000 water molecules; that is, at least 45 water molecules per lipid to ensure a fully hydrated state. The system consisting of a POPC bilayer with 40 mM [H_3O^+] was prepared by randomly replacing 16 water molecules with 16 H_3O^+ ions. For the bulk water systems, 6 H_3O^+ ions were added to a cubic box with ~9000 water molecules. If required, the positive charge of the system was neutralised with Cl^- ions. In all systems Na^+ and Cl^- ions were used to obtain a final concentration of 0.15 M NaCl.

A H_3O^+ concentration of 40 mM is equivalent to approximately a pH of approximately 1.5. For several reasons, we did however not consider changing the protonation state of the phosphate group. Firstly, the pK_a of the phosphate group in phosphatidylcholine lipids depends on the method used and various estimates reported include 0.8[55], <1[56], 1.0[57], 1.3[58], <1.5 [59] and 2.25[38]. Even for the isolated phosphate group, a pK_a value as low as 1.54 has been proposed for dimethyl phosphate [53]. Secondly, these estimates of pK_a rely on critical assumptions that intrinsically limits their accuracy. For example, the pK_a of 0.8 was determined by assuming that the APL is constant and corresponded to that of a fluid-phase phosphatidylcholine bilayer, and that the dielectric permittivity and other properties

of the interfacial water are the same as those of bulk water [60]. There are numerous wet-lab and computational studies showing that interfacial water clearly deviates from that of bulk water [3-7] and variations in pH induce phase transitions in lipid bilayers and alter APL [32-33, 61-62] . Thirdly, given that H_3O^+ ions are likely unequally distributed between the bulk and the membrane surface it is not possible to reliably predict how many of the lipids would be protonated at a given pH. Finally, our previous study of POPC bilayers at low pH have shown that simulations with non-protonated POPC and H_3O^+ ions can qualitatively reproduce the concentration-dependent effect of H_3O^+ ions on APL and membrane thickness [35]. Finally, our study was aimed understanding what happens to properties of water when the membrane is altered by the presence of H_3O^+ ions at the water-lipid interface, rather that understanding the process of protonation or deprotonation, which cannot be described by classical MD.

MD simulation of membrane and 'bulk water' systems at neutral and low pH

All simulations were carried out using GROMACS version 4.6.7 [63], in conjunction with the GROMOS 54A7 force field[64] and parameters for POPC developed by Poger et al. [65] Parameters for the H_3O^+ ion compatible with the GROMOS 54A7 force field were obtained from the Automated Topology Builder (molid 3859). [66-67] Briefly, the partial charges of the oxygen and hydrogen atoms were -0.587*e* and 0.529*e*, respectively, giving an overall charge of +1 to the ion. The O–H bond length and the H–O–H angle were set to 0.0983 nm and 109.50 °, respectively. Water was described using the simple point charge (SPC) model [68]. Temperature and pressure were maintained at 303 K and 1 bar using a Berendsen thermostat and barostat [69].

All systems were simulated using a 2-fs time step. Membrane systems were simulated for 1 *μ*s each and coordinates were saved every 200 ps. As instantaneous position and orientation of water molecules changes at a rate much faster than every 200 ps, each membrane simulation was extended by 40 ns during which the coordinates were saved every 2 ps. All simulations of bulk water were 40-ns long and coordinates were saved every 2 ps. The LINCS algorithm [70] was used to constrain the lengths of all bonds in lipids. Non-bonded interactions were evaluated using a single-range cut-off scheme whereby interactions within a 1.4-nm cut-off were calculated at every step and the pair list was

updated every 5 steps [71]. To correct for the truncation of electrostatic interactions beyond 1.4 nm a reaction-field correction [72] with a relative dielectric constant (ε_r) of 62 was applied. Note that the GROMOS lipid force field parameters were developed with a reaction-field and a single-range cut-off and have been shown to reproduce the structure and dynamics of POPC bilayers.

Simulations of fixed-APL POPC without H_3O^+ ions

Fixed-APL simulations were carried out based on the approach described in Bhide et al [18] , which the authors referred to as a 'frozen' bilayer. The structure from the end of the low pH simulation was chosen as a starting configuration. All H_3O^+ ions and the same number of Cl- ions were removed and this new system was simulated in the NVT ensemble such that the APL remains constant. Analysis showed that after a short time (~5-10 ns) water molecules occupied the space previously filled by the H_3O^+ ions at the water-lipid interface confirming the removal of the ions did not introduce any significant change in the pressure. All other simulations parameters were the same as for the neutral and low pH simulations. The system was simulated for 1 μs.

Data analysis

Analysis was carried out using GROMACS tools[63] and the water dynamics module in the MDAnalysis package [73]. The local density of water as a function of distance from the membrane surface was estimated by counting the number of water molecules in a 0.1 nm thick 'slab' at increasing distances from the water-lipid interface. For this, the water-lipid interface was defined as a plane parallel to the membrane surface in *xy,* and z = 0 being the average *z*-coordinate from all phosphorous atoms in the upper leaflet of the lipid bilayer. For each 'slab' centred at distances between z = -1.5 nm and z = +2.5 nm with respect to the water-lipid interface the number of water molecules were averaged over all frames from the last 500 ns of the 1-*μ*s simulations.

The analysis of the hydrogen bond (H-bond) lifetimes, angular distribution and survival probabilities of water was carried out using the 40-ns trajectory of the membrane

simulations. Similar to the local density, properties were analysed as a function of distance from the membrane surface. However, rather than calculating a given property for all water molecules at a given distance from the membrane surface, made up of all lipid molecules in the upper leaflet, the analysis is carried for water molecules found in a cylindrical volume centred at a selected lipid molecule and at a given distance from the membrane surface in the *z* direction (Figure 1). Compared to averaging properties across all water molecules above the entire membrane surface this approach has the benefit of revealing some of the variations of properties due to the local environment created by the heterogeneous surface of the membrane without explicitly considering the ruggedness of the surface. It also significantly reduces the computational resources required, in particular for properties that are based on an auto-correlation (e.g. orientation relaxation).

The cylindrical volumes used for analysis are illustrated in Figure 1 and were defined as follows. The volume has a radius of 1.5 nm and is positioned at the centre of geometry (COG) of heavy atoms that make up the choline, phosphate and glycerol groups in the selected lipid. The cylinder is positioned at increasing distances away from the water-lipid interface using a lower z value of z = 0, z = 0.5 nm, z = 1.0 nm, z = 1.5 nm, z = 2.0 nm and z = 2.5 nm, where z = 0 is the at the COG of the lipid head group. For example, Figure 1A and 1B show the cylindrical zones of water molecules using a cut-off of z = 0.5 nm and z = 1.0 nm, respectively. For all simulations analysed, the number of water molecules found in this cylindrical zone is between 200 – 400. The property of interest is averaged over all water molecules in the volume and all frames in the simulation. The analysis was carried out for 30 lipid molecules.

To allow for a direct comparison, the analysis for bulk water is carried out a in similar fashion despite there not being a ‘surface’. In this case, water in a cylindrical volume around a selected water molecule is used for analysis. Again, the analysis is repeated for at least 30 water molecules. To ensure this approach does not result in artefacts, all properties were also calculated without the use of layers or cylinder and the property was either averaged over all water in the box or at least 30 water molecules selected at random.

The angular distribution function, also referred to as the orientational polarisation [13], was calculated using the water dynamics module in MDAnalysis. Angular distribution is given as a line histogram of cos(θ) where θ is the angle formed by the dipole vector of a water molecule, $\hat{u}$, and a vector parallel to the *z*-axis of the simulation system, $\hat{n}$. The angular distribution is plotted as a histogram of count(cos(θ)) vs *cos*(θ). Both for the membrane and bulk water the angular distribution was calculated using the cylindrical volumes described above with cut-offs from 0.5 nm to 2.5 nm. For each cut-off, the angular distribution was averaged over 30 values, where each was calculated using a cylindrical volume around a lipid or water molecule selected at random.

The survival probability, as reported by Pu et al [74], was used to estimate how long a set of water molecules remain in a given volume and is defined as

$$P(\tau) = \frac{1}{T}\sum_{t=1}^{T}\frac{N(t, t+\tau)}{N(t)}$$

where T is the maximum time of the simulation, τ is the time-step and N(t) is the number of particles, in the volume of interest, at time t and N(t + τ) is the number of particles at every frame from time t to τ in the same volume. As for the analysis of angular distribution the cylindrical volumes with cut-offs from 0.5 nm to 2.5 nm were used and for each cut-off the survival probability was averaged over 30 values. The survival probability is plotted as $P(\tau)$ vs *t.*

The water orientation relaxation, as reported by Yeh & Mou [75], was used to estimate how fast water molecules are rotating as given by the change in direction of their dipole vector. The corresponding time correlation function is defined as

$$C_{\hat{u}}(\tau) = \langle P_2\,[\hat{u}(t_0)\cdot\,\hat{u}(t_0+\,\tau\,)]\,\rangle$$

where $P_2 = (3x^2 - 1)/2$ is the second-order Legendre polynomial and $\hat{u}$ is the dipole vector of the water molecule.

For H-bond lifetimes, also referred to as hydrogen bond population relaxation, the autocorrelation function as proposed by Rapaport [76] was used. This is given by

$$C(\tau) = \frac{\sum_{ij} h_{ij}(t_0)\, h'_{ij}(t_0 + \tau)}{\sum_{ij} h_{ij}(t_0)}$$

where $h'_{ij}(t_0 + \tau)$ = 1 if there is a continuous H-bond between atom pairs *ij* during the time interval $(t_0 + \tau)$ and $h'_{ij}(t_0 + \tau)$ = 0 otherwise. As for the analysis of angular distribution and survival probability water in cylindrical volumes with cut-offs from 0.5 nm to 2.5 nm were used and for each cut-off, and averaged over 30 values.

For survival probability and H-bond lifetimes, the characteristic relaxation times were obtained by fitting the following two-term exponential:

$$C(t) = A_1 exp\left(\frac{-t}{\tau_1}\right) + A_2 exp\left(\frac{-t}{\tau_2}\right)$$

where A_1 and τ_1 describe the fast component and A_2 and τ_2 describe the slow component.

For the orientational relaxation the curves do not decay to zero within the sampled timeframe and an additional, constant term A3 was added to account for this.

$$C(t) = A_1 exp\left(\frac{-t}{\tau_1}\right) + A_2 exp\left(\frac{-t}{\tau_2}\right) + A_3$$

Results

Water 'layers' at the water-lipid interface

One of the consistent observations from studies of interfacial water is that the density of water is reduced compared to the bulk. Figure 2 shows the density of water as a function of distance to the membrane surface obtained from the neutral and low pH membrane simulations. The density was calculated by counting the number of water molecules in 0.1 nm thick 'slabs' at distances from -01.5 nm to +0.25 nm from the membrane surface, averaged over all frames in the last 500 ns of the simulation. The membrane surface was defined as a plane in the *xy* dimension of the simulation box *z* = 0 being the average *z*-

coordinate from all phosphorous atoms in the upper leaflet of the lipid bilayer (shown as grey spheres in Figure 2). Approximating the bilayer surface by a plane does not account for local variations in the positon of the head groups in the *z* dimension and thus neglects the 'ruggedness' of the bilayer surface. However, over time and space these variations are averaged out, thus having little impact on macroscopic properties such as density. The confirm this, the average z-position of all P atoms in the upper and lower bilayer, averaged over all frames in the last 500 ns of the simulation of POPC in the presence of H_3O^+ was calculated (Figure S1 in the supplementary material). The results from this analysis confirm that, on average, there is no statistically significant difference in the *z*-position of the 256 P atoms that form the bilayer surface (confidence interval 99%). Also, as reported in our previous work [35], the H_3O^+ ions accumulate at the water-lipid interface within ~100 - 150 ns and after that the ions are rarely found in the bulk solution (see also Fig S2 in the supplementary material). As a result, membrane properties such as APL and position of head group atoms that can affect the density of water are equilibrated in the last 500 ns of the simulations that are used for analysis here.

As can be seen from the graphs in Figure 2, the density of water is zero in the hydrophobic part of the membrane and steadily increases until it reaches bulk at ~1 nm from the membrane surface. This is consistent with other studies showing that density of water approaches bulk values at approximately 0.5 to 2.0 nm form the membrane surface [8, 23, 77]. While the graphs from the neutral and low pH simulations show the same shape the one from the low pH simulation is clearly shifted towards the right. As a result, the density at the membrane surface is lower indicating that less water penetrates into the water-lipid interface (z = 0).

Water at the membrane surface in a neutral system

Figure 3 shows different properties of water calculated from simulations of POPC under neutral conditions. As detailed in the methods section, these properties were calculated for five regions, each 0.5 nm wide, at increasing distances from the membrane surface.

These are named region I to IV (see also Figure 1). In addition, the same properties were calculated for bulk water from simulations of a box of water molecules.

Survival probability is a measure of permanence i.e. of how long a water molecule remains in given volume. A slower decay of survival probability indicates that water molecules reside longer time in a given volume. Figure 3A shows average survival probabilities for the five regions in comparison to bulk water. For each region, the data shown is the average $\pm$ standard deviation over 30 lipid molecules, where each average represents an average over time (frames) and water molecules found in the volume surrounding the given lipid molecule. A qualitative comparison of these graphs shows that water molecules closest to the membrane surface (region I) show the longest permanence time, indicated by the slowest decay of the survival probability. Even after 50 ps the survival probability has not reached zero. For each region moving further away from the membrane surface, the permanence time decreases. Quantitatively this is reflected in the relaxation times for the survival probabilities listed in Table 2. Analysis showed that a two-component exponential gave a much better fit than a single exponential, in particular for the two regions closest to the bilayer. This means there exists a fast and a slow component of the decay. The relaxation time for the slow component, given by τ_2, ranges from 22.1 ps for water closest to the membrane (region I) to 4.7 ps for water in the region furthest away from the membrane (V). Similarly, τ_2 describing the relaxation time of the fast component, ranges from 3.1 ps for region I to 0.8 ps for region V. Both the slow and fast components indicate that water in or near the lipid headgroup experiences a drastic slowing down compared to water closer towards the bulk. Both the fast and slow component of the relaxation times decrease by an approximate order of magnitude when water moves from region I to V. The biggest change in relaxation time is clearly seen when water moves into (or out of) the region closest to the membrane. Also, comparison to values from bulk water show that even at distance of 2.5 nm from the surface, the permanence time of water is still affected by the membrane surface. The survival probabilities for the 30 individual data sets of each region are shown in Figure S3 in the supplementary material. From this, and the error bars on the average survival

probabilities in Fig 3A, it is evident that the variability of survival probabilities within a given region is much larger for water close to the membrane than water towards the bulk.

Our findings are consistent with previous reports from simulations of phospholipid bilayers [8, 19]. For example, Debnath et al reported MD simulations of DPPC bilayers and analysis of the survival probabilities and their relaxation times showed that τ for the fast and slow components are 19.2 ps and 1.4 ps for water that continuously reside within +/- 0.3 nm of the phosphate atoms. These values are comparable to the ones reported in this study. Like in our study, τ is reduced ~10 fold for water that approaches bulk (defined as water that continuously reside >1.5 nm above the phosphate atoms). Another study by Bhide et al from simulations of DOPC and DOPS bilayers showed the same trends [8].

Next, we compare the H-bond lifetimes for the different water regions. Figure 3B and Table 3 show the decay for the H-bond lifetimes and the corresponding relaxation times. The decay of the lifetimes seen in Figure 3B suggests that it is mostly the water buried in the lipid head groups (region I) that is affected. This is confirmed by the relaxation times. The slow component, $\tau_{2,}$ is 3.9 ps and 1.5 ps, respectively, for water in regions I and II, which is ~4 and 2 time larger than for bulk water. For water that is > 1.0 nm away from the membrane surface τ_2 is comparable to the value from bulk water. Thus, in comparison to survival probability, only the water molecules in the two closest regions to the membrane deviate from bulk water.

The water orientation relaxation estimates how fast water molecules change direction. A slow decay of orientational relaxation indicates that a water molecule remains in the same orientation for longer compared to water molecules with a fast decay. Figure 3C shows the orientational relaxation for the five water regions and Table 4 lists the characteristic relaxation times. The decay was fitted to a two-component exponential that contains an additional, constant term (A_3), to account for the decay not reaching zero in some of the regions. Comparison of the A_3 values from the different regions shows an increased value for regions I and II. This indicates an orientation preference for the dipole of water molecules buried in, and just above, the lipid head groups on a time-scale longer than the

20 ps. A_3 continually decreases for each region further away and reaches bulk values for water > 2.0 nm from the membrane surface, indicating a loss of this orientation preference. The relaxation times τ_1 and τ_2 show that the times between reorientation of the dipole is significantly increased for waters < 1.5 nm from the membrane surface. This indicates that the closer the water is to the lipid head groups the longer it spends in a given orientation. The nature of this preference is described in more detail in the section on the analysis of the angular distribution.

The slowdown of the water dipole orientation agrees with results from previously reported studies of interfacial water. For example, Bhide et al [18] carried out simulations of DOPC bilayers and separated water molecules into regions based on whether they were part of the first solvation shell of lipids or not. For water that are continuously found close to lipid headgroups the orientational correlation function is substantially reduced compared to bulk water. The effect is reduced but still present for water that is located just above the lipid head group. Similarly, Murzyn et al [20] showed that the reorientation of water molecules within 0.4 nm of any atom of a POPC lipid bilayer is strongly reduced and the effect is gradually lost for water > 0.7 – 1.2 nm from the membrane surface. Further, the nonzero decay of water buried in the lipid head group observed in our simulations agrees with previous results from Debnath et al [19].

As noted above, the nonzero decay of the water orientation relaxation indicates an orientational preference. This can be quantified by the angular distribution for the water dipole vector. Figure 3D shows the angular distribution for the five interfacial water regions and bulk water. Angular distribution is given as a line histogram of $\cos(\theta)$ vs θ where θ is the angle formed by the dipolar vector and a vector parallel to the *z*-axis of the simulation system (which is the normal to the membrane surface that runs along the *xy* plane). Values of $\cos(\theta) = -1$ and $\cos(\theta) = 1$, mean the water dipole is parallel to the membrane normal (i.e. perpendicular to the membrane surface). In the case of $\cos(\theta) = -1$ the dipole is pointing towards the membrane surface and in the case of $\cos(\theta) = 1$ the dipole is pointing away from the surface. At $\cos(\theta) = 0$, the dipole is at right angle to the membrane normal i.e. the dipole runs parallel to the membrane surface. A flat line for

cos(θ) vs θ implies that all orientations are equally likely meaning the water dipole does not show a preferred orientation.

Comparison of the angular distribution from the five regions shows that for region I, the water dipole is strongly affected and exhibits a high preference for values close to cos(θ) = -1. This signifies that the dipole is preferentially orientated almost parallel to the membrane normal and pointing towards the membrane surface. As can be seen from the angular distribution of the other regions, this preference gradually reduces to zero as water approaches bulk. For water, just above the lipid head groups (region II), this preference is still present but much reduced compared to water closest to the lipid head group. For water that is > 1.0 nm from the surface the preference is essentially lost, indicated by the flat line histograms. These observations are consistent with results from spectroscopy experiments with different phospholipid bilayers showing that, on average, the dipole of interfacial water molecules points towards the membrane surface[9, 11, 14] and that water molecules become more and more randomized as they move towards bulk solution [14].

In summary, the data from our simulations of water at the interface of a POPC lipid bilayer under neutral conditions reproduce previously reported findings of increased permanence times, increased H-bond lifetimes, reduced orientational relaxation, and a preferred orientation of the water dipole. The results also show that these changes are most pronounced for water buried in the lipid headgroups and gradually decrease for water further away from the membrane surface.

Water at the membrane surface in a low pH system

For a direct comparison to a POPC bilayer under neutral conditions, the survival probability, H-bond lifetimes, orientational relaxation and angular distribution were calculated from simulations of POPC at low pH (i.e. in the presence of H_3O^+ ions). The results from this analysis are shown in Figure 4. Comparison of the survival probability from the simulations of POPC under neutral conditions (Figure 3A) and at low pH (Figure 4A) shows that in the presence of H_3O^+ ions the decay of the survival probability for all

five regions is shifted further away from the bulk. Specifically, the survival probability for each of five regions shows a slower decay in the presence of H_3O^+ compared to the neutral condition. Quantitatively, this can be seen in the relaxation times shown in Table 5. Comparing the slow component of the decay, $\tau_{2,}$ from the neutral system (Table 2) to τ_2 from the low pH system (Table 5) shows that in the latter, τ_2 increases by ~80% for all regions of interfacial water. For example, for water molecules closest to the water-lipid interface, τ_2 increases from 22.1 ps under neutral conditions to 38.8 ps at low pH. The values for $\tau_{1,}$ show an increase of ~30% suggesting that the fast component of the decay is less affected by the presence of H_3O^+ than the slow component. Besides these increases in permanence time, the overall trend between the regions is the same. That is, the biggest change in τ_1 and τ_2 occurs from region I to region II and the change becomes successively smaller the further away water is from the membrane surface. Overall, the results from the survival probability analysis indicate that permanence time of interfacial water is much higher in the presence of H_3O^+.

Figure 4B and Table 6 show H-bond lifetimes and corresponding decay times calculated from the low pH simulations. Comparison of the H-bond lifetimes from the neutral and low pH system show that similar to survival probability, all curves are moved away further away from the bulk value. In the case of the H-bond lifetimes the effect is however less pronounced. Comparison of the H-bond relaxation times from neutral conditions (Table 3) and low pH (Table 6) shows that in the latter the slow component of the decay (τ_2) is increased in all five regions while the fast component (τ_1) is not affected much. Like in the survival probably, the overall trend between the five regions is the same at neutral and low pH.

Figure 4C shows the time-dependent decay of the orientational relaxation obtained from the low pH simulations. Both the decay curves and the values of A_3 suggest that in the presence of H_3O^+ not only region I but also region II shows a non-zero decay. This implies that water molecules in both these regions show a marked orientational preference. Also, compared to neutral conditions, at low pH none of the five regions reach the decay seen in bulk. Figure 4D shows the angular distribution plots for low pH simulations. Like in the

neutral system, the waters in region I show a strong preference for cos(θ) = -1 indicating that for the majority of water molecules the dipole is pointing towards the membrane surface. However, in contrast to the neutral system, at low pH there is no gradual decrease of this preference for water further away from the membrane surface. Water in region II shows an almost flat distribution suggesting that, on average, water molecules in region II show no preferred orientation. Region III shows a small preference for cos(θ) = 1 where the dipole points away from the membrane surface.

In summary, comparison of water at the surface of a POPC lipid bilayer under neutral conditions and at low pH suggests that for the latter, the changes in the properties of interfacial water deviate even more from the ones in bulk water. The most pronounced difference is for the survival probabilities and orientational relaxation. In addition, the presence of H_3O^+ ions affects the orientation of the dipole.

Direct and indirect contributions from H_3O^+ estimated from 'fixed-APL' simulations

The combined results from this and previous studies suggest that H_3O^+ ions affect both the structure of the membrane itself and that of interfacial water. As noted in the introduction, the interplay of the membrane, interfacial water and surface-bound ions is complex and most effects are interrelated and hard to isolate. Even in our simple model system of limited complexity, there are different ways in which the presence of H_3O^+ ions can induce changes in the properties of interfacial water. Either directly, *via* water-H_3O^+ interactions, or, indirectly, *via* the H_3O^+-induced lowering of APL. To isolate the indirect effect of APL from the direct effect of water-H_3O^+ on the different properties, we carried out additional simulations of a 'fixed-APL' bilayer without H_3O^+ ions. In these simulations, the membrane shows the same reduced APL as seen in the low pH simulations, but without the explicit presence of H_3O^+.

From these simulations, all properties were calculated using the same approach as for the neutral and low pH simulation systems. Comparison of the survival probabilities, H-bond lifetimes and orientation relaxation shows that qualitatively the interfacial water behaves in the same manner as in the simulations of POPC in the absence and presence

of H_3O^+ ions. That is, the water closest to the membrane surface (region I) shows the strongest deviation from bulk and the effect gradually decrease for water further away from the membrane surface (Figures S4A, S4B and S4C in the supplementary material). Comparison of the decay for these three properties (Tables S1, S2 and S3 in the supplementary material) shows that for region I the value of τ_2 is approximately halfway between the values from the simulations of POPC in absence and presence of H_3O^+ ions. For all other regions, the decay times are either the same or close to the values from simulations under neutral conditions. Similarly, for the orientation relaxation, the constant term (A_3) that accounts for the decay not reaching zero, obtained from the fixed-APL simulations is also approximately in between the values from the neutral and low pH simulations (Table S3).

Comparison of the angular distribution from the fixed-APL simulations (Figure S4D) to the ones from the neutral (Figure 3D) and low pH simulation (Figure 4D) shows that the orientation of the water molecules in the fixed-APL is closer to the one found at low pH than under neutral conditions. Like in the simulation of POPC at low pH, the fixed-APL simulations lack the gradual decrease of preferred orientations that is seen in simulations of POPC under neutral conditions, and only the water molecules in region I show a preferred orientation.

Discussion

In this study, we aimed to investigate the effect of H_3O^+ ions on the structure and dynamics of interfacial water. For this, we carried out extensive MD simulation of a solvated POPC lipid bilayer (at full hydration) under conditions mimicking neutral pH and low pH. In a previous study [35], we have used such simulations to demonstrate the effect of H_3O^+ ions on the structure and morphology of the bilayer. Results showed that H_3O^+ ions accumulate at the water-lipid interface where they form strong and long-lived H-bonds with the phosphate and carbonyl oxygens of the lipids (see also Fig S2 in the supplementary material). As a result of these lipid-H_3O^+ interactions the bilayer shows a reduced APL and increased membrane thickness, compared to the same bilayer in the absence of H_3O^+ ions. This condensing of the bilayer agrees with the results from neutron

scattering and electrical impedance spectroscopy experiments of POPC at low pH [34]. Results presented in the current study suggests that the presence of H_3O^+ also affects the structure and dynamics of interfacial water. As noted, our previous study[35] showed that our model to describe H_3O^+ interacting with POPC bilayers can qualitatively predict the effect of H_3O^+ ions on APL and membrane thickness. Nevertheless, it is worth noting that describing the solvated proton as a H_3O^+ ion, and thus ignoring the presence of Eigen and/or Zundel cations, presents a limitation of our model with respect to the detailed interaction of a solvated proton with interfacial water molecules. For this reason, we focus our analysis on macroscopic properties, averaged over large number of water molecules as well as time, and the comparison of these averages between neutral and low pH conditions, rather than in terms of specific molecular interactions of individual water and H_3O^+ ions.

There are numerous wet-lab and simulation studies demonstrating that the properties of interfacial water deviate from that of bulk water [1-2, 4, 40-41]. Central to the study of interfacial water is the concept of layers where water is organised in distinct, but connected regions [2, 8, 12-15, 18-20, 22-23, 77-80]. The number and definition of layers varies and depends, among others, on the properties investigated and/or the techniques used. This means it is often not possible to do a direct, quantitative comparison of results from different studies. Nevertheless, in most studies, interfacial water is considered to be between 1 – 2 nm form the membrane surface.

In agreement with this, analysis of water at the surface of a POPC bilayer under neutral conditions reveals that, compared to bulk water, interfacial water exhibits increased permanence, reduced orientational relaxation, longer-lived H-bonds and a preferred orientation in which the water dipole points towards the membrane surface. For all properties, the deviation from bulk is the largest for water closest to the water-lipid interface (region I). The effect is gradually reduced as the distance to the membrane increases. As described in the relevant results sections, these observations agree with previously reported data. It is interesting to note that the distance at which the water returns to bulk values depends on the property. For example, the survival probability

deviates from bulk for water as far as 2.5 nm from the membrane surface. In contrast, the orientational relaxation and H-bond lifetimes only deviate from bulk values for water within 0.5 nm and 1 nm of the membrane surface, respectively. Similarly, only water within 1 nm of the membrane surface shows preferred orientation. A possible reason for this is that survival probability is affected by all of the other properties as well as the diffusion of interfacial water, which has been shown to deviate from bulk water different diffusion [8, 13, 20, 23-24].

Comparison of data from the simulation of POPC at neutral and low pH shows all of these properties are affected by the presence of H_3O^+ ions but the extent of the effect differs. For example, at low pH, the permanence time for all five regions is slowed down even further away from bulk water than for neutral conditions. In particular, the slow component of the decay of the survival probability is strongly affected by the presence of H_3O^+. Similar effects are seen in orientational relaxation and H-bond lifetimes. As a consequence of these effects, the layer in which the properties of water deviate from bulk appears to grow thicker. In their study on the orientational motion of water at the interface of a DOPC bilayer, Bhide et al [18] noted the challenges of interpreting the mechanisms underlying the different timescales in the orientational relaxation of interfacial water. Nevertheless, in a previous studies [81] of water in a confined space, the three timescales in the decay of the orientational relaxation were interpreted as follows using a 'wobbling-in-a-cone' model: the first (fast) component is related to the relaxation of the fast internal-librational motion. The authors noted in their study that this motion was too fast to be observed in the experiments. [81] The second, intermediate timescale corresponds to the relaxation of the molecules' restricted motion inside the cone while the third and slowest timescale relates to the full relaxation of the orientation (i.e. the relaxation *of* the cone) in which the water returns to its unrestricted motion. Furthermore, based on the results from their 'frozen' simulations, Bhide et al [18] noted that one of the reasons for the slowing down of the orientational relaxation for water close to the interface is the motion of the headgroup lipid. However, even if this motion is removed the water still does not reach relaxation times seen in bulk water. Based on simulations of phosphatidylcholine lipid bilayers it is not really possible to separate the contribution of the choline or phosphate groups to this

effect due to their coupled motion. Nevertheless, the results from our present study show that the slow component corresponding to the relaxation of the cone itself is further reduced in the presence of H_3O^+ compared to neutral conditions.

The results from the angular distribution (Figures 3D and 4D) suggest that at low pH the orientational preference of water close to the membrane (region I and II) is reduced, indicating that water is less ordered. At the same time the increase in the non-zero decay of the orientation relaxation for these regions (term A_3 in Tables 4 and 7, and Figures 3C and 4D) suggests a slower reorientation and higher orientational preference. To explain this apparent contradiction, it should be noted that while both angular distribution and orientation relaxation are related to the orientation of the water molecules with respect to the membrane surface, the two properties are not the same. Also, they occur and are measured at very different timescales. Orientational relaxation measures how fast water molecules are rotating given by the change in direction of their dipole vector and the decay time of this process occurs on the time scale of a few to 10s of ns. In contrast, angular distribution is a measure of orientational preference of the dipole with respect to the membrane surface. This is obtained from averaging the position of the water dipole over 100s of ns. Based on the combined results it appears that at low pH, individual water molecules are slowed down in their rotation but over longer time frames and averaged over many water molecules the preferred orientation is reduced.

Previous studies using vibrational sum frequency generation spectroscopy (VSFG) [11] show that addition of $CaCl_2$ reduces ordering of interfacial water at the surface of a zwitterionic DPPC bilayer. Based on the comparison of VSFG spectra from DPPC in the absence and presence of $CaCl_2$ the authors propose that the Ca^{2+} shields the charge of the phosphate and as a result reduces the impact of the P-N dipole of the lipid headgroup on the water. It has also been shown previously that Ca^{2+} binds to the surface of phospholipid bilayers and interacts with phospholipid head groups and, like H_3O^+, reduces the APL of the bilayer. Based on these similarities and the higher charge density of H_3O^+ ions, it is possible that the decrease in the preferred orientation of water close to a membrane surface in the presence of H_3O^+ is caused by a similar effect. However, to

directly assess this a direct comparison of the same system with and without Ca^{2+} at low and high pH is needed, which is beyond the scope of this study.

As noted before the observed changes in the properties of interfacial water at low pH can be caused directly by the interaction of H3O+ with water or indirectly by the H_3O^+-induced lowering of APL. The fixed-APL simulations allowed us to isolate these effects. If the direct interaction of H_3O^+ ions with interfacial water were the only contribution to the differences seen in the neutral or low pH systems, interfacial water in the fixed-APL simulations (where the H_3O^+ ions were removed) should exhibit the same patterns and values as in the neutral POPC simulations. On the other hand, if the reduced APL is the main contribution to the observed differences of interfacial water at neutral and low pH, properties in the fixed-APL simulations would be equal or close to values from simulations of POPC in the presence H_3O^+ (even if the ions themselves have been removed). As the results from fixed-APL simulations show, the contributions from these different effects depends on the property. Results from the survival probabilities, H-bond lifetimes and orientation relaxation shows that for water closest to the membrane surface (region I) the decay times of the slow components are in-between the values for simulations in the absence and presence of H_3O^+ ions. This suggests that for water molecules that are located in the lipid headgroups, the same region where H_3O^+ ions are found, the increase in survival time and H-bond lifetimes seen in simulations of POPC in the presence of H_3O^+ is a result of both the reduced APL and the direct water- H_3O^+ interactions. Furthermore, for all other regions, the values are the same or close to the ones from simulations under neutral conditions. Thus, in the absence of direct interaction with H_3O^+ ions, the reduced APL itself, does not affect survival probabilities and H-bond lifetimes of the interfacial water. Results from the angular distribution analysis shows that the orientation of the water molecules in the fixed-APL is closer to the one found at low pH than under neutral conditions. This indicates that the tighter packing of the lipids, induced by the lipid-H_3O^+ interactions, is the main contribution to the changes in the orientation of interfacial water molecules.

As noted in the introduction, acidic pH affects the properties of phospholipid bilayers including the lamellar gel-to-liquid crystalline phase-transition temperature or membrane conductance and capacitance. This suggests a tighter packing of lipids, consistent with the reduced APL and increased membrane thickness seen in experiments and simulations [34-35], caused by the direct interaction of the hydronium ions [35, 51-53]. One can also speculate that some of these changes in membrane properties are more indirectly caused by the changes in interfacial water at low pH. For example, the widening of the interfacial water layer and the increase in ordering of water at low pH might stabilise the gel phase and thus contribute to the observed increase of the lamellar gel-to-liquid crystalline phase-transition temperature. Another example, of how interfacial effects can alter membrane properties was reported by Zhou and Raphael [32] who showed that pH-induced changes in bending stiffness resulted from alterations of interfacial electrostatics as opposed to changes in the intramembrane dipole potential. Results from these studies highlight the complex interplay of interracial water and membrane properties. Nevertheless, to assess if and how the pH-induced changes in interfacial water affect biological processes requires studies on more complex membranes that better mimic cell membranes

Summary and conclusion

While numerous studies investigated the properties of interfacial water little is known if and how these properties are affected by the presence of H_3O^+ ions, as found at low pH. To address this question, we used extensive MD simulations to compare the structure and dynamics of water at the interface of a POPC bilayer, in the absence and presence of H_3O^+ ions. Analysis of properties using five different water layers, at increasing distance from the membrane surface, highlights that the distance at which the water deviates from bulk depends on the property. Under the neutral conditions, the survival probability of interfacial water appears to be affected for water as far as 2.5 nm from the membrane surface while orientational relaxation, H-bond lifetimes and orientational preference only deviate for the water within about 0.5 – 1 nm from lipid headgroups. Likewise, the extent to which properties are affected by the presence of H_3O^+ varies. Most affected is the survival probability, which is much higher in the presence of H_3O^+ than under neutral

conditions. Similarly, H_3O^+ slows down the orientational relaxation even further compared to neutral conditions. Independent of the extent of the deviation from bulk, in all three properties the H_3O^+ ions cause the long-range effect to extend further away from the membrane surface. In the case of the angular distribution, the H_3O^+ ions appear to reduce the preferred orientation. Results from fixed-APL simulations in the absence of H_3O^+ suggest that the tighter packing of the lipids, induced by the lipid-H_3O^+ interactions, rather than the direct water-H_3O^+ interactions, are the major contribution to the changes in the dipole orientation of interfacial water molecules. In contrast, the changes in survival probability and H-bond lifetimes are likely a combination of the direct interaction of H3O+ ions with water as well as the reduced APL.

Supporting Information

Average *z*-position of P atoms in the upper and lower leaflets of a POPC bilayer in the presence of H_3O^+ ions; Position of H_3O^+ ions in the simulation system of POPC with H_3O^+ ions; Survival probability for the five regions of interfacial water under neutral conditions; Properties of interfacial water from 'fixed-APL' simulations of membranes in the absence of H_3O^+; Relaxation times for survival probabilities of interfacial water from the 'fixed-APL' simulations and for bulk water in the absence of H_3O^+; Relaxation times for H-bond lifetimes of interfacial water from the 'fixed-APL' simulations and for bulk water in the absence of H_3O^+. Relaxation times for orientation lifetimes of interfacial water from the 'fixed-APL' simulations and for bulk water in the absence of H_3O^+.

at the start of the simulation (t = 0 ns), randomly placed in the simulation system, and after 200 ns of simulation as they accumulate at the water-lipid interface.

Acknowledgments

E.D would like to thank Dr Alvaro Garcia and Adj Prof Bruce Cornell from the University of Technology Sydney for insightful discussions, and Mr Alejandro Bernardin, Universidad de Valparaíso, for assistance with the water analysis scripts in MDAnalysis. This work was supported by resources provided by the Pawsey Supercomputing Centre with funding from the Australian Government and the Government of Western Australia, as

well as with the assistance of resources provided at the NCI National Facility systems at the Australian National University through the National Computational Merit Allocation Scheme supported by the Australian Government.

Conflict of interest

The authors declare no competing financial interest.

References

1. Disalvo, E. A., Membrane Hydration: A Hint to a New Model for Biomembranes. In *Membrane hydration: The role of water in the structure and function of biological membranes*, Disalvo, E. A., Ed. Springer International Publishing: Cham, 2015; pp 1-16.
2. Disalvo, E. A.; Lairion, F.; Martini, F.; Tymczyszyn, E.; Frias, M.; Almaleck, H.; Gordillo, G. J., Structural and functional properties of hydration and confined water in membrane interfaces. *Biochimica et biophysica acta* **2008,** *1778* (12), 2655-70.
3. Balasubramanian, S.; Pal, S.; Bagchi, B., Hydrogen-bond dynamics near a micellar surface: Origin of the universal slow relaxation at complex aqueous interfaces. *Phys. Rev. Lett.* **2002,** *89* (11), 115505.
4. Berkowitz, M. L.; Vácha, R., Aqueous solutions at the interface with phospholipid bilayers. *Acc. Chem. Res.* **2012,** *45* (1), 74-82.
5. Milhaud, J., New insights into water–phospholipid model membrane interactions. *BBA Biomembranes* **2004,** *1663* (1), 19-51.
6. Pasenkiewicz-Gierula, M.; Baczynski, K.; Markiewicz, M.; Murzyn, K., Computer modelling studies of the bilayer/water interface. *BBA Biomembranes* **2016,** *1858* (10), 2305-2321.
7. Watanabe, N.; Suga, K.; Umakoshi, H., Functional hydration behavior: Interrelation between hydration and molecular properties at lipid membrane interfaces. *J. Chem.* **2019,** *2019*, 15.
8. Bhide, S. Y.; Berkowitz, M. L., Structure and dynamics of water at the interface with phospholipid bilayers. *J. Chem. Phys.* **2005,** *123* (22), 224702.
9. Binder, H., Water near lipid membranes as seen by infrared spectroscopy. *Eur. Biophys. J.* **2007,** *36* (4-5), 265-79.
10. Klose, G.; Arnold, K.; Peinel, G.; Binder, H.; Gawrisch, K., The structure and dynamics of water near membrane surfaces. *Colloids Surf.* **1985,** *14* (1), 21-30.
11. Chen, X.; Hua, W.; Huang, Z.; Allen, H. C., Interfacial water structure associated with phospholipid membranes studied by phase-sensitive vibrational sum frequency generation spectroscopy. *J. Am. Chem. Soc.* **2010,** *132* (32), 11336-11342.
12. Jedlovszky, P.; Mezei, M., Orientational order of the water molecules across a fully hydrated DMPC bilayer: A Monte Carlo simulation study. *J. Phys. Chem. B* **2001,** *105* (17), 3614-3623.
13. Marrink, S. J.; Berkowitz, M.; Berendsen, H. J. C., Molecular dynamics simulation of a membrane/water interface: the ordering of water and its relation to the hydration force. *Langmuir* **1993,** *9* (11), 3122-3131.
14. Nagata, Y.; Mukamel, S., Vibrational sum-frequency generation spectroscopy at the water/lipid interface: molecular dynamics simulation study. *J. Am. Chem. Soc.* **2010,** *132* (18), 6434-6442.

15. Yeghiazaryan, G. A.; Poghosyan, A. H.; Shahinyan, A. A., The water molecules orientation around the dipalmitoylphosphatidylcholine head group: A molecular dynamics study. *Physica A.* **2006,** *362* (1), 197-203.
16. Zhou, Z.; Sayer, B. G.; Hughes, D. W.; Stark, R. E.; Epand, R. M., Studies of phospholipid hydration by high-resolution magic-angle spinning Nuclear Magnetic Resonance. *Biophys. J* **1999,** *76* (1), 387-399.
17. Mondal, J. A.; Nihonyanagi, S.; Yamaguchi, S.; Tahara, T., Three distinct water structures at a zwitterionic lipid/water interface revealed by heterodyne-detected vibrational sum frequency generation. *J. Am. Chem. Soc.* **2012,** *134* (18), 7842-7850.
18. Bhide, S. Y.; Berkowitz, M. L., The behavior of reorientational correlation functions of water at the water-lipid bilayer interface. *J. Chem. Phys.* **2006,** *125* (9), 094713.
19. Debnath, A.; Mukherjee, B.; Ayappa, K. G.; Maiti, P. K.; Lin, S. T., Entropy and dynamics of water in hydration layers of a bilayer. *J. Chem. Phys.* **2010,** *133* (17), 174704.
20. Murzyn, K.; Zhao, W.; Karttunen, M.; Kurdziel, M.; Róg, T., Dynamics of water at membrane surfaces: Effect of headgroup structure. *Biointerphases* **2006,** *1* (3), 98-105.
21. Pal, S. K.; Sukul, D.; Mandal, D.; Sen, S.; Bhattacharyya, K., Solvation dynamics of DCM in micelles. *Chem. Phys. Lett.* **2000,** *327* (1), 91-96.
22. Zhang, Z.; Berkowitz, M. L., Orientational dynamics of water in phospholipid bilayers with different hydration levels. *J. Phys. Chem. B* **2009,** *113* (21), 7676-7680.
23. Das, J.; Flenner, E.; Kosztin, I., Anomalous diffusion of water molecules in hydrated lipid bilayers. *J. Chem. Phys.* **2013,** *139* (6), 065102.
24. Róg, T.; Murzyn, K.; Pasenkiewicz-Gierula, M., The dynamics of water at the phospholipid bilayer surface: a molecular dynamics simulation study. *Chem. Phys. Lett.* **2002,** *352* (5), 323-327.
25. Chan, Y.-H. M.; Boxer, S. G., Model membrane systems and their applications. *Curr. Opin. Chem. Biol.* **2007,** *11* (6), 581-587.
26. Dror, R. O.; Dirks, R. M.; Grossman, J. P.; Xu, H.; Shaw, D. E., Biomolecular simulation: A computational microscope for molecular biology. *Annu. Rev. Biophys.* **2012,** *41* (1), 429-452.
27. Fragneto, G., Neutrons and model membranes. *Eur. Phys. J. Spec. Top.* **2012,** *213* (1), 327-342.
28. Ingólfsson, H. I.; Melo, M. N.; van Eerden, F. J.; Arnarez, C.; Lopez, C. A.; Wassenaar, T. A.; Periole, X.; de Vries, A. H.; Tieleman, D. P.; Marrink, S. J., Lipid organization of the plasma membrane. *J. Am. Chem. Soc.* **2014,** *136* (41), 14554-14559.
29. Mashaghi, A.; Mashaghi, S.; Reviakine, I.; Heeren, R. M. A.; Sandoghdar, V.; Bonn, M., Label-free characterization of biomembranes: from structure to dynamics. *Chem. Soc. Rev.* **2014,** *43* (3), 887-900.
30. Molugu, T. R.; Lee, S.; Brown, M. F., Concepts and methods of solid-state NMR spectroscopy applied to bomembranes. *Chem. Rev.* **2017,** *117* (19), 12087-12132.
31. Umegawa, Y.; Matsumori, N.; Murata, M., Recent solid-state NMR studies of dydrated lipid membranes. In *Ann. Rep. NMR Spectro.*, Webb, G. A., Ed. Academic Press: 2018; Vol. 94, pp 41-72.
32. Zhou, Y.; Raphael, R. M., Solution pH alters mechanical and electrical properties of phosphatidylcholine membranes: relation between Interfacial electrostatics, intramembrane potential, and bending elasticity. *Biophys. J* **2007,** *92* (7), 2451-2462.
33. Koynova, R.; Caffrey, M., Phases and phase transitions of the phosphatidylcholines. *BBA Biomembranes* **1998,** *1376* (1), 91-145.
34. Cranfield, C. G.; Berry, T.; Holt, S. A.; Hossain, K. R.; Le Brun, A. P.; Carne, S.; Al Khamici, H.; Coster, H.; Valenzuela, S. M.; Cornell, B., Evidence of the key role of H3O+ in phospholipid membrane morphology. *Langmuir* **2016,** *32* (41), 10725-10734.
35. Deplazes, E.; Poger, D.; Cornell, B.; Cranfield, C. G., The effect of hydronium ions on the structure of phospholipid membranes. *Phys. Chem. Chem. Phys.* **2018,** *20* (1), 357-366.

36. Naumowicz, M.; Figaszewski, Z. A., The effect of pH on the electrical capacitance of phosphatidylcholine-phosphatidylserine system in bilayer lipid membrane. *J. Membr. Biol.* **2014,** *247* (4), 361-369.
37. Petelska, A. D.; Figaszewski, Z. A., Effect of pH on the interfacial tension of bilayer lipid membrane formed from phosphatidylcholine or phosphatidylserine. *BBA Biomembranes* **2002,** *1561* (2), 135-146.
38. Gutman, M.; Nachliel, E., The dynamic aspects of proton transfer processes. *BBA Bioenergetics* **1990,** *1015* (3), 391-414.
39. Heberle, Proton transfer reactions across bacteriorhodopsin and along the membrane. *BBA Bioenergetics* **2000,** *1458* (1), 135-147.
40. Mulkidjanian, A. Y.; Cherepanov, D. A., Probing biological interfaces by tracing proton passage across them. *Photochem. Photobiol. Sci.* **2006,** *5* (6), 577-87.
41. Mulkidjanian, A. Y.; Heberle, J.; Cherepanov, D. A., Protons @ interfaces: implications for biological energy conversion. *Biochim Biophys Acta* **2006,** *1757* (8), 913-30.
42. Antonenko, Y. N.; Pohl, P., Microinjection in combination with microfluorimetry to study proton diffusion along phospholipid membranes. *Eur. Biophys. J.* **2008,** *37* (6), 865-70.
43. Cherepanov, D. A.; Junge, W.; Mulkidjanian, A. Y., Proton transfer dynamics at the membrane/water interface: dependence on the fixed and mobile pH buffers, on the size and form of membrane particles, and on the interfacial potential barrier. *Biophys. J* **2004,** *86* (2), 665-80.
44. Antonenko, Y. N.; Kovbasnjuk, O. N.; Yaguzhinsky, L. S., Evidence in favor of the existence of a kinetic barrier for proton transfer from a surface of bilayer phospholipid membrane to bulk water. *BBA Biomembranes* **1993,** *1150* (1), 45-50.
45. Georgievskii, Y.; Medvedev, E. S.; Stuchebrukhov, A. A., Proton transport via the membrane surface. *Biophys. J* **2002,** *82* (6), 2833-2846.
46. Deplazes, E.; White, J.; Murphy, C.; Cranfield, C. G.; Garcia, A., Competing for the same space: protons and alkali ions at the interface of phospholipid bilayers. *Biophys. Rev.* **2019,** *11* (3), 483-490.
47. Brändén, M.; Sandén, T.; Brzezinski, P.; Widengren, J., Localized proton microcircuits at the biological membrane-water interface. *Proc. Natl. Acad. Sci. U. S. A.* **2006,** *103* (52), 19766-19770.
48. Sandén, T.; Salomonsson, L.; Brzezinski, P.; Widengren, J., Surface-coupled proton exchange of a membrane-bound proton acceptor. *Proc. Natl. Acad. Sci. U. S. A.* **2010,** *107* (9), 4129-4134.
49. Springer, A.; Hagen, V.; Cherepanov, D. A.; Antonenko, Y. N.; Pohl, P., Protons migrate along interfacial water without significant contributions from jumps between ionizable groups on the membrane surface. *Proc. Natl. Acad. Sci. U. S. A.* **2011,** *108* (35), 14461-6.
50. Weichselbaum, E.; Osterbauer, M.; Knyazev, D. G.; Batishchev, O. V.; Akimov, S. A.; Hai Nguyen, T.; Zhang, C.; Knor, G.; Agmon, N.; Carloni, P.; Pohl, P., Origin of proton affinity to membrane/water interfaces. *Sci. Rep.* **2017,** *7* (1), 4553.
51. Smondyrev, A. M.; Voth, G. A., Molecular dynamics simulation of proton transport through the influenza A virus M2 channel. *Biophys. J* **2002,** *83* (4), 1987-96.
52. Wolf, M. G.; Grubmuller, H.; Groenhof, G., Anomalous surface diffusion of protons on lipid membranes. *Biophys. J* **2014,** *107* (1), 76-87.
53. Yamashita, T.; Voth, G. A., Properties of hydrated excess protons near phospholipid bilayers. *J. Phys. Chem. B* **2010,** *114* (1), 592-603.
54. Deplazes, E.; Poger, D.; Cornell, B.; Cranfield, C. G., The effect of hydronium ions on the structure of phospholipid membranes. *Phys. Chem. Chem. Phys.* **2017,** *20* (1), 357-366.
55. Pasenkiewicz-Gierula, M.; Takaoka, Y.; Miyagawa, H.; Kitamura, K.; Kusumi, A., Charge pairing of headgroups in phosphatidylcholine membranes: A molecular dynamics simulation study. *Biophys. J* **1999,** *76* (3), 1228-1240.

56. London, E.; Feigenson, G. W., Phosphorus NMR analysis of phospholipids in detergents. *J. Lipid Res.* **1979,** *20*, 408-412.
57. Pasenkiewicz-Gierula, M.; Takaoka, Y.; Miyagawa, H.; Kitamura, K.; Kusumi, A., Hydrogen bonding of water to phosphatidylcholine in the membrane as studied by a molecular dynamics simulation: location, geometry, and lipid−lipid bridging via hydrogen bonded water. *J. Phys. Chem. A* **1997,** *101* (20), 3677-3691.
58. Fernández, M. S.; Calderón, E., Surface Ionization of dipalmitoylphosphatidylcholine as detected by the pH dependence of the phase transition temperature of liposomes. *Berichte der Bunsengesellschaft für physikalische Chemie* **1991,** *95* (12), 1669-1674.
59. Eibl, H.; Woolley, P., Electrostatic interactions at charged lipid membranes. Hydrogen bonds in lipid membrane surfaces. *Biophys. Chem.* **1979,** *10* (3), 261-271.
60. Moncelli, M. R.; Becucci, L.; Guidelli, R., The intrinsic pKa values for phosphatidylcholine, phosphatidylethanolamine, and phosphatidylserine in monolayers deposited on mercury electrodes. *Biophys. J* **1994,** *66* (6), 1969-1980.
61. Träuble, H.; Eibl, H., Electrostatic Effects on Lipid Phase Transitions: Membrane Structure and Ionic Environment. *Proc. Natl. Acad. Sci. U. S. A.* **1974,** *71*, 214-219.
62. Siegel, D. P.; Burns, J. L.; Chestnut, M. H.; Talmon, Y., Intermediates in membrane fusion and bilayer/nonbilayer phase transitions imaged by time-resolved cryo-transmission electron microscopy. *Biophys. J* **1989,** *56* (1), 161-169.
63. Hess, B.; Kutzner, C.; Van Der Spoel, D.; Lindahl, E., GROMACS 4: algorithms for highly efficient, load-balanced, and scalable molecular simulation. *J. Chem. Theory Comput.* **2008,** *4* (3), 435-447.
64. Schmid, N.; Eichenberger, A. P.; Choutko, A.; Riniker, S.; Winger, M.; Mark, A. E.; van Gunsteren, W. F., Definition and testing of the GROMOS force-field versions 54A7 and 54B7. *Eur Biophys J* **2011,** *40* (7), 843-856.
65. Poger, D.; Van Gunsteren, W. F.; Mark, A. E., A new force field for simulating phosphatidylcholine bilayers. *J. Comp. Chem.* **2010,** *31* (6), 1117-1125.
66. Koziara, K. B.; Stroet, M.; Malde, A. K.; Mark, A. E., Testing and validation of the Automated Topology Builder (ATB) version 2.0: prediction of hydration free enthalpies. *J. Comput. Aid. Mol. Des.* **2014,** *28* (3), 221-233.
67. Malde, A. K.; Zuo, L.; Breeze, M.; Stroet, M.; Poger, D.; Nair, P. C.; Oostenbrink, C.; Mark, A. E., An Automated force field Topology Builder (ATB) and repository: Version 1.0. *J. Chem. Theory Comput.* **2011,** *7* (12), 4026-4037.
68. Berendsen, H. J. C.; Postma, J. P. M.; van Gunsteren, W. F.; Hermans, J., Interaction models for water in relation to protein hydration. In *Intermolecular Forces*, Pullman, B., Ed. Springer Netherlands: 1981; Vol. 14, pp 331-342.
69. Berendsen, H. J. C.; Postma, J. P. M.; van Gunsteren, W. F.; Dinola, A.; Haak, J. R., Molecular dynamics with coupling to an external bath. *J. Chem. Phys.* **1984,** *81* (8), 3684-3690.
70. Hess, B.; Bekker, H.; Berendsen, H. J. C.; Fraaije, J. G. E. M., LINCS: A linear constraint solver for molecular simulations. *J. Comp. Chem.* **1997,** *18* (12), 1463-1472.
71. Reißer, S.; Poger, D.; Stroet, M.; Mark, A. E., Real cost of speed: The effect of a time-saving multiple-time-stepping algorithm on the accuracy of molecular dynamics simulations. *J. Chem. Theory Comput.* **2017**.
72. Tironi, I. G.; Sperb, R.; Smith, P. E.; van Gunsteren, W. F., A generalized reaction field method for molecular dynamics simulations. *J. Chem. Phys.* **1995,** *102* (13), 5451-5459.
73. Michaud-Agrawal, N.; Denning, E. J.; Woolf, T. B.; Beckstein, O., MDAnalysis: A toolkit for the analysis of molecular dynamics simulations. *J. Comp. Chem.* **2011,** *32* (10), 2319-2327.
74. Liu, P.; Harder, E.; Berne, B. J., On the calculation of diffusion coefficients in confined fluids and interfaces with an application to the liquid−vapor interface of water. *J. Phys. Chem. B* **2004,** *108* (21), 6595-6602.

75. Yeh, Y.-l.; Mou, C.-Y., Orientational relaxation dynamics of liquid water studied by molecular dynamics simulation. *J. Phys. Chem. B* **1999,** *103* (18), 3699-3705.
76. Rapaport, D. C., Hydrogen bonds in water. *Mol. Phys.* **1983,** *50* (5), 1151-1162.
77. Pandit, S. A.; Bostick, D.; Berkowitz, M. L., An algorithm to describe molecular scale rugged surfaces and its application to the study of a water/lipid bilayer interface. *J. Chem. Phys.* **2003,** *119* (4), 2199-2205.
78. Krylov, N. A.; Pentkovsky, V. M.; Efremov, R. G., Nontrivial behavior of water in the vicinity and inside lipid bilayers as probed by molecular dynamics simulations. *ACS nano* **2013,** *7* (10), 9428-42.
79. Nickels, J. D.; Katsaras, J., Water and lipid bilayers. In *Membrane hydration: The role of water in the structure and function of biological membranes*, Disalvo, E. A., Ed. Springer International Publishing: Cham, 2015; pp 45-67.
80. Zhao, W.; Moilanen, D. E.; Fenn, E. E.; Fayer, M. D., Water at the surfaces of aligned phospholipid multibilayer model membranes probed with ultrafast vibrational spectroscopy. *J. Am. Chem. Soc.* **2008,** *130* (42), 13927-13937.
81. Tan, H.-S.; Piletic, I. R.; Fayer, M. D., Orientational dynamics of water confined on a nanometer length scale in reverse micelles. *J. Chem. Phys.* **2005,** *122* (17), 174501.
82. Poger, D.; Mark, A. E., Lipid bilayers: The effect of force field on ordering and dynamics. *J. Chem. Theory Comput.* **2012,** *8* (11), 4807-4817.

Figures and Tables

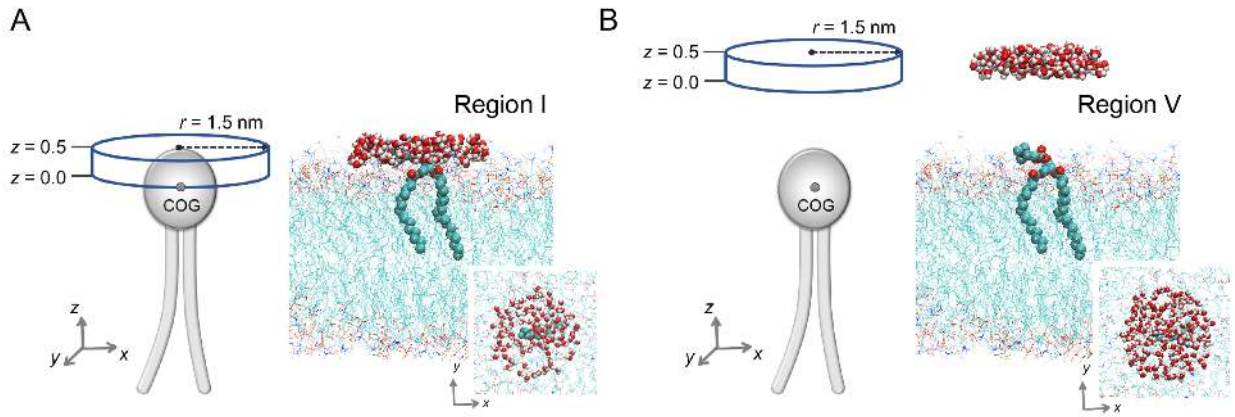

Figure 1. Schematic of cylindrical volumes used for analysis of interfacial water. Five groups of water molecules were selected by defining a cylindrical volume around a selected lipid molecule at five different, increasing distances away from the water-lipid interface. For this, the cylinder was positioned at z = 0 – 0.5 nm (region I), z = 0.5 – 1.0 nm (region II), z = 1.0 – 1.5 nm (region III), z = 1.5 – 2.0 nm (region VI), z = 2.0 – 2.5 nm (region V), where z = 0 is the at the centre of geometry (COG) of the heavy atoms in the head group of the selected lipid. (A) and (B) show the cylindrical volume and the resulting group of water molecules for regions I and V, respectively. The small inset image shows the same group of water molecules from a 'top view' i.e. looking down onto the membrane surface.

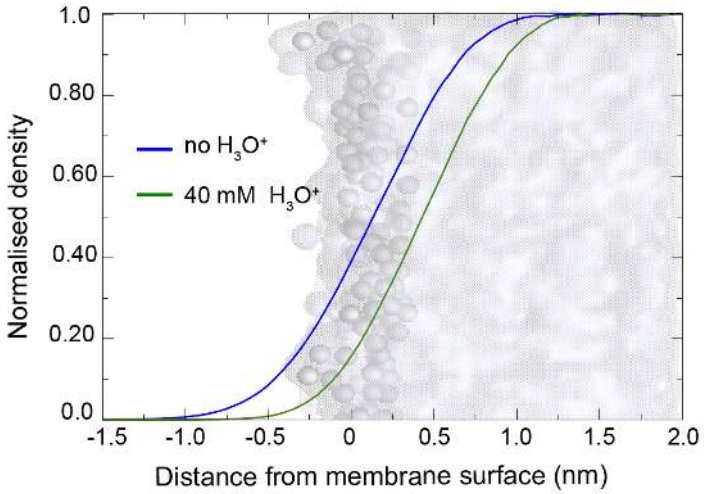

Figure 2: Normalised density of water as a function of distance from the membrane surface, calculated from simulations of POPC bilayers in the absence and presence of H_3O^+. The density was calculated from the last 500 ns of a 1-μs simulation of POPC without H_3O^+ ions (blue) and in the presence of 40 mM [H_3O^+] (green).

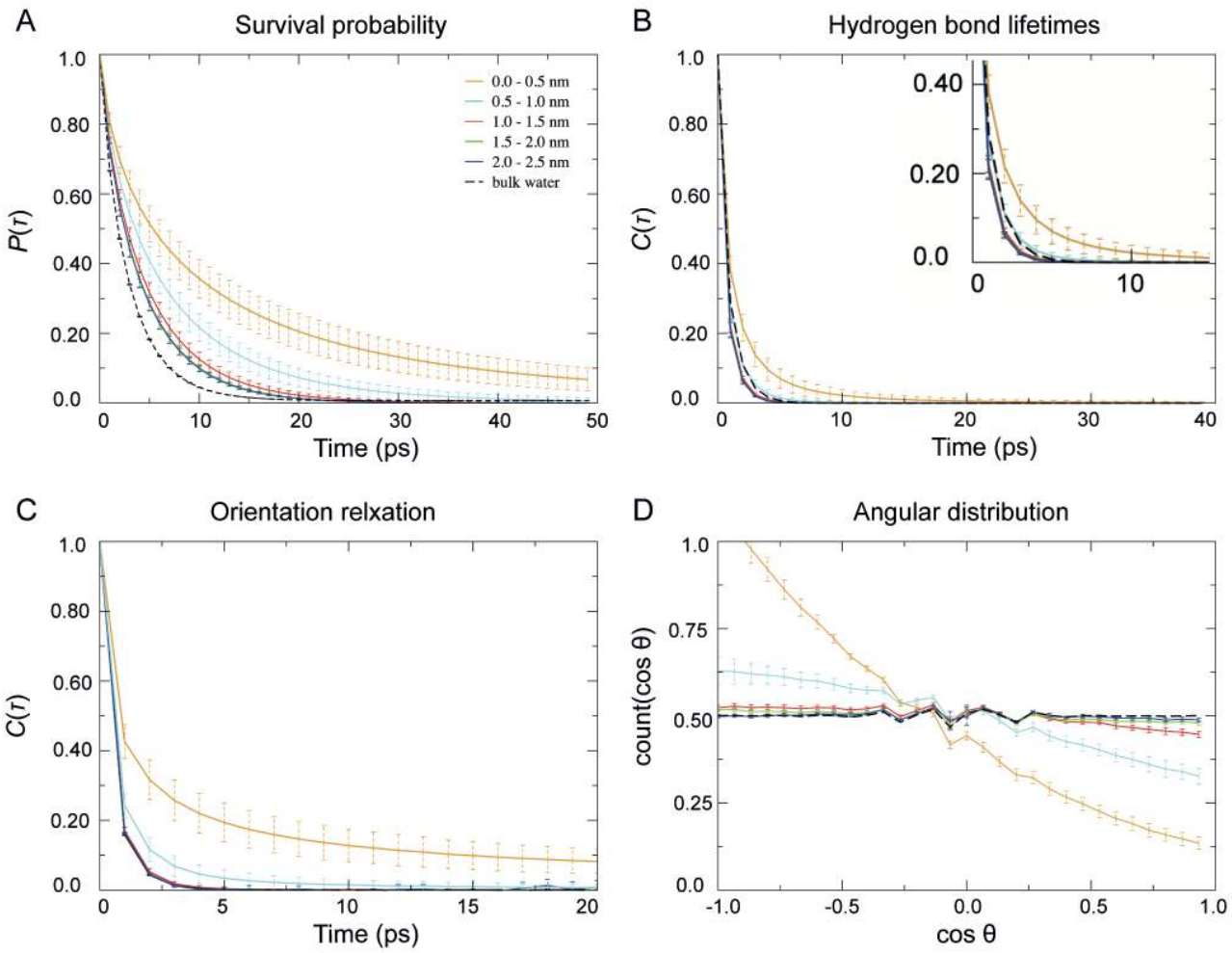

Figure 3. Properties of interfacial water from simulations of POPC under neutral conditions. (A) survival probability, (B) hydrogen bond lifetimes, (C) orientation relaxation and (D) angular distribution for five regions, at increasing distances from the membrane surface. As reference the same property from simulations of bulk water is shown (black). Error bars are 1 standard deviation. For all plots the five regions are: z = 0 – 0.5 nm (region I, orange), z = 0.5 – 1.0 nm (region II, cyan), z = 1.0 – 1.5 nm (region III, red), z = 1.5 – 2.0 nm (region IV, green), z = 2.0 – 2.5 nm (region V, blue), where z = 0 is the at the centre of geometry of head group of the selected lipid (see also Figure 1).

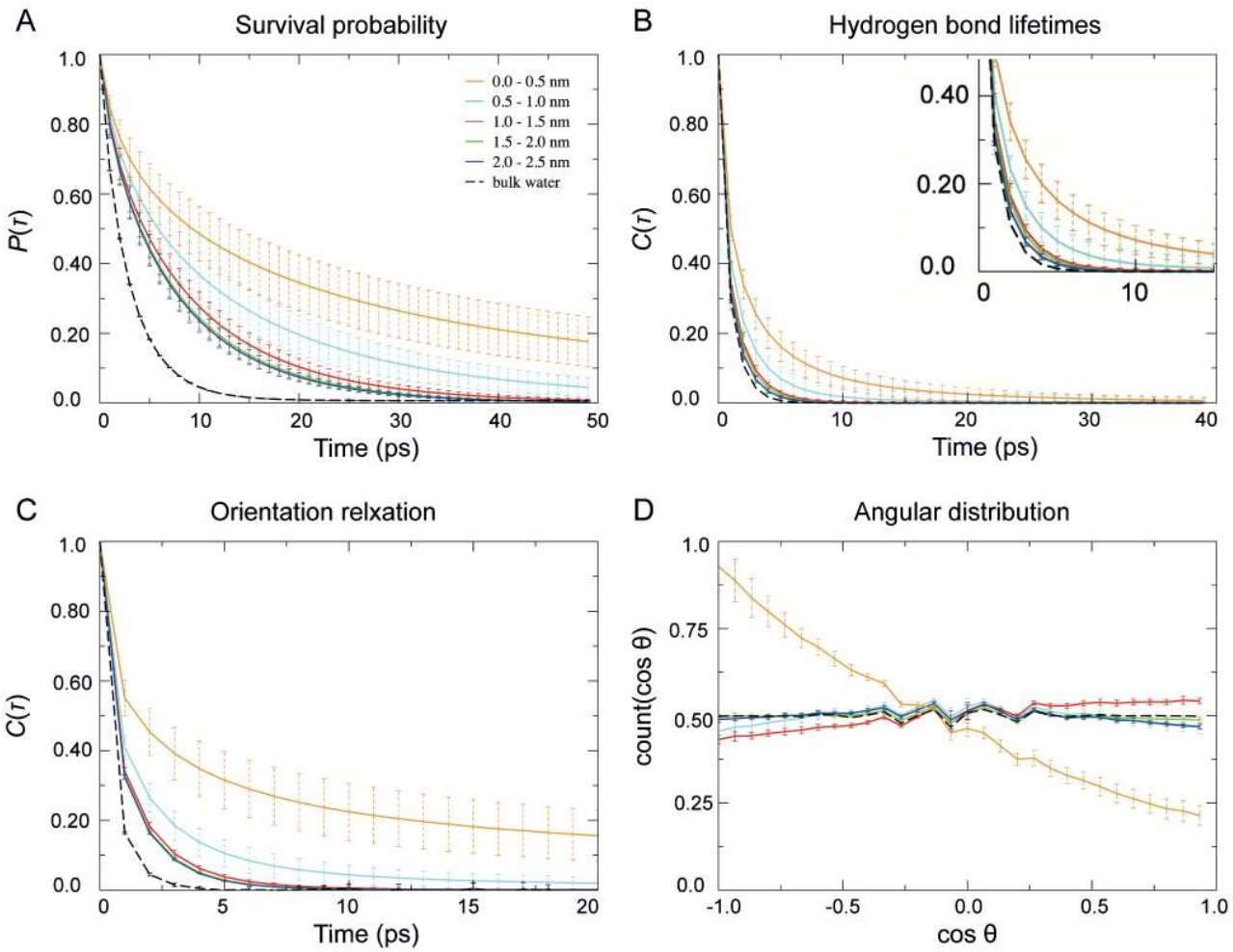

Figure 4. Properties of interfacial water from simulations of POPC in the presence of 40 mM H_3O^+. (A) survival probability, (B) hydrogen bond lifetimes, (C) orientation relaxation and (D) angular distribution for five regions, at increasing distances from the membrane surface. As reference the same property from simulations of bulk water is shown (black). Error bars are 1 standard deviation. For all plots the five regions are: z = 0 – 0.5 nm (region I, orange), z = 0.5 – 1.0 nm (region II, cyan), z = 1.0 – 1.5 nm (region III, red), z = 1.5 – 2.0 nm (region IV, green), z = 2.0 – 2.5 nm (region V, blue), where z = 0 is the at the centre of geometry of head group of the selected lipid (see also Figure 1).

Table 1: Overview of simulation systems, the corresponding number of H_3O^+ ions added, the resulting H_3O^+ concentrations and simulations times. For membrane simulations, the angular distribution and density was calculated from the last 500 ns of a 1-μs simulation. Survival probability, orientational relaxation and H-bond lifetimes were calculated from a 40-ns simulation where frames were written out every 2 ps. Data for the POPC bilayer in the absence of H_3O^+ ions were taken from a previous study [65, 82]

System		**Number of H_3O^+ ions**	**[H_3O^+]**	**Simulations**
Membrane	Neutral	-	-	1 µs, 40 ns
	Low pH	16	40 mM	1 µs, 40 ns
	Fixed-APL	-	-	1 µs, 40 ns
Bulk water	Neutral	-	-	40 ns
	Low pH	6	40 mM	40 ns

Table 2. Relaxation times for survival probabilities of interfacial water and bulk water under neutral conditions. For each of the five regions as well as for bulk water, relaxation times were obtained by fitting a two-term exponential decay to the corresponding survival probabilities. A_1 and τ_1 describe the fast component and A_2 and τ_2 describe the slow component. For all fits the correlation coefficients were > 0.99 and Chi2 was < $3*10^{-3}$.

Region	A_1	τ_1 **(ps)**	A_2	τ_2 **(ps)**
0.0 – 0.5 nm (I)	0.5	3.1	0.5	22.1
0.5 – 1.0 nm (II)	0.3	1.9	0.6	9.2
1.0 – 1.5 nm (III)	0.2	1.1	0.8	5.5
1.5 – 2.0 nm (IV)	0.2	1.0	0.8	4.8
2.0 – 2.5 nm (V)	0.2	1.0	0.8	4.7
Bulk water	0.1	0.8	0.8	3.2

Table 3. Relaxation times for H-bond lifetimes of interfacial water and bulk water under neutral conditions. For each of the five regions as well as for bulk water, relaxation times were obtained by fitting a two-term exponential decay to the corresponding H-bond lifetime curves. A_1 and τ_1 describe the fast component and A_2 and τ_2 describe the slow component. For all fits the correlation coefficients were > 0.99 and Chi2 was < $5*10^{-4}$.

Region	A_1	τ_1 **(ps)**	A_2	τ_2 **(ps)**
0.0 – 0.5 nm (I)	0.7	0.7	0.3	3.9
0.5 – 1.0 nm (II)	0.6	0.5	0.4	1.5
1.0 – 1.5 nm (III)	0.5	0.4	0.5	1.0
1.5 – 2.0 nm (IV)	0.4	0.3	0.6	0.9
2.0 – 2.5 nm (V)	0.4	0.3	0.6	0.8
Bulk water	0.3	0.3	0.7	0.9

Table 4. Relaxation times for orientation relaxation of interfacial water and bulk water under neutral conditions. For each of the five regions as well as for bulk water, relaxation times were obtained by fitting a two-term exponential decay to the corresponding orientation relaxation curves. A_1 and τ_1 describe the fast component and A_2 and τ_2 describe the slow component. The constant term A_3 accounts for the decay of some regions not reaching zero within the sampling time. For all fits the correlation coefficients were > 0.99 and Chi2 was < $8*10^{-5}$.

Region	A_1	τ_1 **(ps)**	A_2	τ_2 **(ps)**	A_3
0.0 – 0.5 nm (I)	0.6	0.5	0.3	5.1	0.082
0.5 – 1.0 nm (II)	0.8	0.5	0.2	2.1	0.009
1.0 – 1.5 nm (III)	0.6	0.3	0.3	0.9	0.0008
1.5 – 2.0 nm (IV)	0.4	0.3	0.3	0.8	0.0003
2.0 – 2.5 nm (V)	0.4	0.3	0.3	0.7	0.0001
Bulk water	0.0	0.4	0.1	0.8	0.0001

Table 5. Relaxation times for survival probabilities of interfacial water and bulk water in the presence of H_3O^+. For each of the five regions as well as for bulk water, relaxation times were obtained by fitting a two-term exponential decay to the corresponding survival probabilities curves. A_1 and τ_1 describe the fast component and A_2 and τ_2 describe the slow component. For all fits the correlation coefficients were > 0.99 and Chi2 was < $3*10^{-3}$.

Region	A_1	τ_1 **(ps)**	A_2	τ_2 **(ps)**
0.0 – 0.5 nm (I)	0.4	3.6	0.6	38.8
0.5 – 1.0 nm (II)	0.3	2.6	0.6	17.5
1.0 – 1.5 nm (III)	0.2	1.6	0.7	10.1
1.5 – 2.0 nm (IV)	0.2	1.4	0.7	8.7
2.0 – 2.5 nm (V)	0.2	1.4	0.7	8.4
Bulk water	0.2	0.8	0.8	3.3

Table 6. Relaxation times for H-bond lifetimes of interfacial water and bulk water in the presence of H_3O^+. For each of the five regions as well as for bulk water, relaxation times were obtained by fitting a two-term exponential decay to the corresponding H-bond lifetime curves. A_1 and τ_1 describe the fast component and A_2 and τ_2 describe the slow component. For all fits the correlation coefficients were > 0.99 and Chi2 was < $2*10^{-3}$.

Region	A_1	τ_1 **(ps)**	A_2	τ_2 **(ps)**
0.0 – 0.5 nm (I)	0.7	0.9	0.3	7.1
0.5 – 1.0 nm (II)	0.6	0.6	0.4	3.1
1.0 – 1.5 nm (III)	0.5	0.4	0.5	1.7
1.5 – 2.0 nm (IV)	0.4	0.4	0.6	1.6
2.0 – 2.5 nm (V)	0.4	0.4	0.5	1.4
Bulk water	0.3	0.3	0.7	1.0

Table 7. Relaxation times for orientation relaxation of interfacial water and bulk water in the presence of H_3O^+. For each of the five regions as well as for bulk water, relaxation times were obtained by fitting a two-term exponential decay to the corresponding orientation relaxation curves. A_1 and τ_1 describe the fast component and A_2 and τ_2 describe the slow component. The constant term A_3 accounts for the decay of some regions not reaching zero within the sampling time. For all fits the correlation coefficients were > 0.99 and Chi2 was < $2*10^{-4}$.

Region	A_1	τ_1 **(ps)**	A_2	τ_2 **(ps)**	A_3
0.0 – 0.5 nm (I)	0.4	0.5	0.4	5.9	0.14
0.5 – 1.0 nm (II)	0.8	0.5	0.2	3.1	0.02
1.0 – 1.5 nm (III)	0.4	0.4	0.5	1.8	0.002
1.5 – 2.0 nm (IV)	0.4	0.4	0.5	1.6	0.0008
2.0 – 2.5 nm (V)	0.4	0.4	0.5	1.6	0.0008
Bulk water	0.6	0.3	0.3	0.9	0.0001

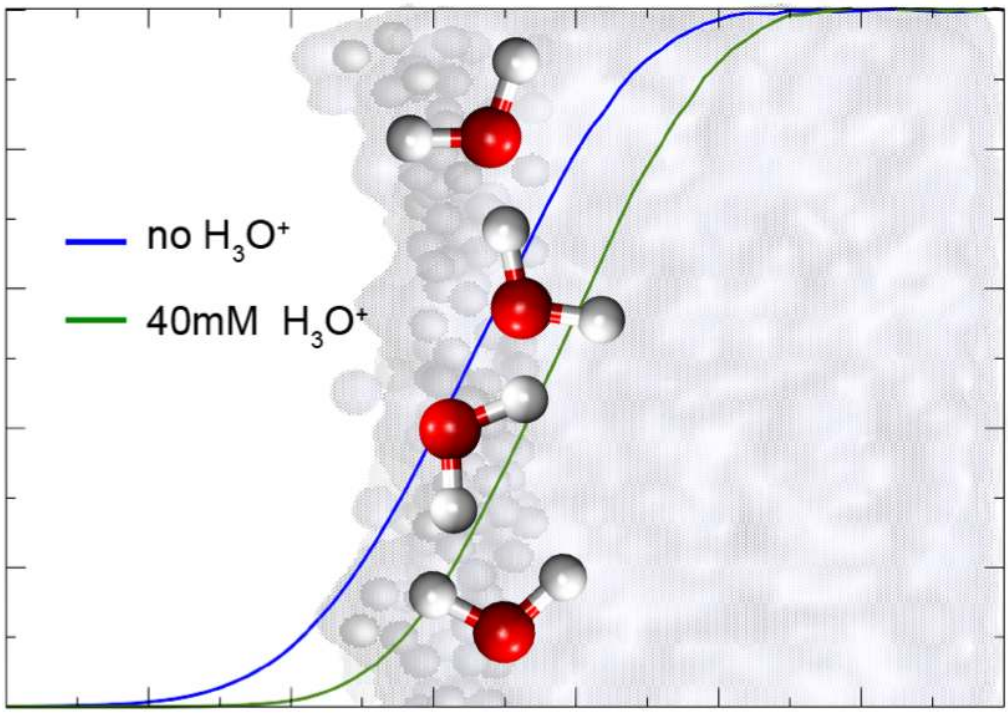
no H_3O^+
40mM H_3O^+